PUBLICATIONS

Online: ISSN 2008-949X

# **Journal of Mathematics and Computer Science**



Journal Homepage: www.isr-publications.com/jmcs

## Jacobi polynomials on a novel subclass of bi-univalent functions for advanced image processing applications



Baskaran Sudharsanan<sup>a</sup>, Saravanan Gunasekar<sup>b</sup>, Timilehin Gideon Shaba<sup>c,\*</sup>, Lakhdar Ragoub<sup>d</sup>, Daniel Breaz<sup>e</sup>, Luminiṭa-Ioana Cotîrlă<sup>f</sup>

#### **Abstract**

This study explores a novel category of bi-univalent functions within the open unit disk, defined through subordination principles and linked to Jacobi polynomials. By utilizing the structural properties of these classical orthogonal polynomials, we derive sharp bounds for the initial Taylor-Maclaurin coefficients, specifically  $|\tau_2|$  and  $|\tau_3|$ , for functions within this subclass. Furthermore, we establish a Fekete-Szegö type inequality involving the functional  $|\tau_3-\rho\tau_2^2|$ , where  $\rho$  is a real parameter. The results obtained generalize and extend various known results in the context of bi-univalent function theory. Notably, this framework has potential applications in image enhancement, where the derived function classes contribute to improved edge detection, feature preservation, and contrast adjustment. Incorporating Jacobi polynomials enhances the theoretical framework while showcasing the method's strength and versatility in processing and improving various image types.

**Keywords:** Bi-univalent functions, Jacobi polynomials, image enhancement, Jacobi polynomial convolution enhancement algorithm (JPCEA).

2020 MSC: 30C45, 30C80.

©2026 All rights reserved.

#### 1. Introduction and preliminary

We define the set of all normalized analytic functions as A. These functions, represented as f(z), have the form

$$\mathbf{f}(z) = z + \sum_{j=2}^{\infty} \tau_j z^j, \quad (z \in \mathbb{D}), \tag{1.1}$$

Email addresses: sbas9991@gmail.com (Baskaran Sudharsanan), gsaran825@yahoo.com (Saravanan Gunasekar), gsaran825@yahoo.com (Timilehin Gideon Shaba), 1.ragoub@upm.edu.sa (Lakhdar Ragoub), dbreaz@uab.ra (Daniel Breaz), luminita.cotirla@math.utcluj.ro (Luminița-Ioana Cotîrlă)

doi: 10.22436/jmcs.041.03.03

Received: 2025-05-14 Revised: 2025-06-26 Accepted: 2025-07-28

<sup>&</sup>lt;sup>a</sup>Department of Mathematics, Dwaraka Doss Goverdhan Doss Vaishnav College (Autonomous), Chennai, 600106, Tamilnadu, India.

<sup>&</sup>lt;sup>b</sup>PG and Research Department of Mathematics, Pachaiyappa's College, Chennai- 600030, Tamil Nadu, India.

<sup>&</sup>lt;sup>c</sup>Department of Mathematics and Statistics, Redeemer's University, Ede 232101, Nigeria.

<sup>&</sup>lt;sup>d</sup>Mathematics Department, University of Prince Mugrin, P.O. Box 41040, Al Madinah 42241, Saudi Arabia.

<sup>&</sup>lt;sup>e</sup>Department of Mathematics, "1 Decembrie 1918" University of Alba Iulia, 510009 Alba Iulia, Romania.

<sup>&</sup>lt;sup>f</sup>Department of Mathematics, Technical University of Cluj-Napoca, 400114 Cluj-Napoca, Romania.

<sup>\*</sup>Corresponding author

where  $\mathbb{D} := \{z \in \mathbb{C} : |z| < 1\}$ . We define S as the subclass of  $\mathcal{A}$  that consists of univalent functions. For  $h_1(z)$  and  $h_2(z)$  in  $\mathcal{A}$ ,  $h_1(z)$  is considered subordinate to  $h_2(z)$  if there exists a function  $\zeta(z)$  such that  $\zeta(0) = 0$ ,  $|\zeta(z)| < 1$  in  $\mathbb{D}$ , and  $h_1(z) = h_2(\zeta(z))$ . This relationship is expressed as  $h_1(z) \prec h_2(z)$ .

A function f(z) belonging to S is classified as bi-univalent if its inverse,  $f^{-1}(w)$ , can be analytically continued within the region |w| < 1 in the w-plane. The set of all bi-univalent functions in  $\mathbb D$  is denoted by  $\sigma$ . If  $f^{-1}(w)$  is of the form

$$\mathtt{f}^{-1}(w) = w + \sum_{\mathtt{j}=2}^{\infty} \upsilon_{\mathtt{j}} w^{\mathtt{j}}, \quad (w \in \mathbb{D}),$$

then we have

$$\mathbf{f}^{-1}(w) = w - \tau_2 w^2 + (2\tau_2^2 - \tau_3)w^3 - (5\tau_2^3 - 5\tau_2\tau_3 + \tau_4)w^4 + \cdots, \ w \in \mathbb{D}.$$

The concept of bi-univalent functions was first proposed by Lewin [8] in 1967, who derived an upper bound for the second Taylor-Maclaurin coefficient in this class, showing that  $|\tau_2| < 1.51$ . Subsequently, Brannan and Clunie refined this estimate [5], who demonstrated that  $|\tau_2| \leq \sqrt{2}$ . Since then, numerous studies have focused on deriving coefficient bounds for bi-univalent functions (see [4, 12–17, 19] for related developments).

The Fekete-Szegö functional addresses the problem of determining the sharp bounds for expressions of the form  $|\tau_3 - \rho \tau_2^2|$  within a compact class of analytic functions. In particular, when  $\rho=1$ , this expression corresponds to the Schwarzian derivative, a quantity of fundamental importance in the geometric theory of analytic functions. For non-negative  $j, j+\varepsilon, j+\eta, (j\in\mathbb{N}\cup\{0\})$ , a generating function of Jacobi polynomials is defined by

$$\mathfrak{J}_{\mathbf{j}}(\mathbf{y},\mathbf{z}) = \frac{2^{\epsilon+\eta}}{\mathbf{M}(1-\mathbf{y}+\mathbf{M})^{\epsilon}(1+\mathbf{y}+\mathbf{M})^{\eta}},$$

where  $M = M(y,z) = (1-2yz+z^2)^{\frac{1}{2}}$ ,  $\varepsilon > -1$ ,  $\eta > -1$ ,  $y \in [-1,1]$  (see [6, 7]). For a fixed y, the function  $\mathfrak{J}_{j}(y,z)$  is analytic in  $\mathbb{D}$  and is represented by the Taylor series expansion as follows:

$$\mathfrak{J}_{\mathbf{j}}(\mathbf{y},z) = \sum_{\mathbf{j}=0}^{\infty} \mathfrak{N}_{\mathbf{j}}^{(\epsilon,\eta)}(\mathbf{y}) z^{\mathbf{j}},$$

where  $\mathcal{N}_{j}^{(\varepsilon,\eta)}(y)$  is the Jacobi polynomial of degree j. The Jacobi polynomial  $\mathcal{N}_{j}^{(\varepsilon,\eta)}(y)$  satisfies a second-order linear homogeneous differential equation:

$$(1-y^2)\chi'' + (\eta - \varepsilon - (\varepsilon + \eta + 2)y)\chi' + j(j + \varepsilon + \eta + 1)\chi = 0.$$

Jacobi polynomials can alternatively be characterized by the following recursive relationships:

$$\mathcal{N}_{j+1}^{(\varepsilon,\eta)}(y)=(c_jy+d_j)\mathcal{N}_{j}^{(\varepsilon,\eta)}(y)+e_j\mathcal{N}_{j-1}^{(\varepsilon,\eta)}(y),\quad j\geqslant 1,$$

where

$$\begin{split} c_j &= \frac{(2j+\varepsilon+\eta+2)(2j+\varepsilon+\eta+1)}{2(j+1)(j+\varepsilon+\eta+1)},\\ d_j &= \frac{(2j+\varepsilon+\eta+1)(\varepsilon^2-\eta^2)}{2(j+1)(j+\varepsilon+\eta+1)(2j+\varepsilon+\eta)},\\ e_j &= -\frac{(2j+\varepsilon+\eta+2)(j+\varepsilon)(j+\eta)}{(j+1)(j+\varepsilon+\eta+1)(2j+\varepsilon+\eta)} \end{split}$$

with the initial values

$$\mathcal{N}_0^{(\epsilon,\eta)}(y) = 1$$
,

$$\begin{split} \mathcal{N}_{1}^{(\varepsilon,\eta)}(y) &= \frac{1}{2} \left( \varepsilon - \eta + (\varepsilon + \eta + 2) \, y \right), \\ \mathcal{N}_{2}^{(\varepsilon,\eta)}(y) &= \frac{1}{8} \left( (\varepsilon - \eta)^2 - (\varepsilon - \eta) - 4 + 2(\varepsilon - \eta)(\varepsilon + \eta + 3) y + (\varepsilon + \eta + 3)(\varepsilon + \eta + 4) y^2 \right). \end{split} \tag{1.2}$$

Table 1 shows the special cases of  $\mathcal{N}_{j}^{(\varepsilon,\eta)}(y)$  and Figure 1 shows the Image of  $\mathbb{D}$  under  $\mathfrak{J}_{j}(y,z)$ .

TE 1 1 4 0	. 1 (		1 . 1			1	
Table 1: S	nacial to	orme i	darivad	trom	12COh1	noliti	nomiale
Table 1. J	Deciai i	omino i	uerreu	110111	acobi	POIVE	ionnais

S. No.	Condition	Corresponding Special Polynomial
1	$\epsilon = \eta = 0$	Legendre polynomials
2	$\varepsilon = \eta = -0.5$	Chebyshev polynomials (first kind)
3	$\varepsilon = \eta = 0.5$	Chebyshev polynomials (second kind)
4	$\epsilon=\eta$	Gegenbauer polynomials (with $\varepsilon - 0.5$ substitution)

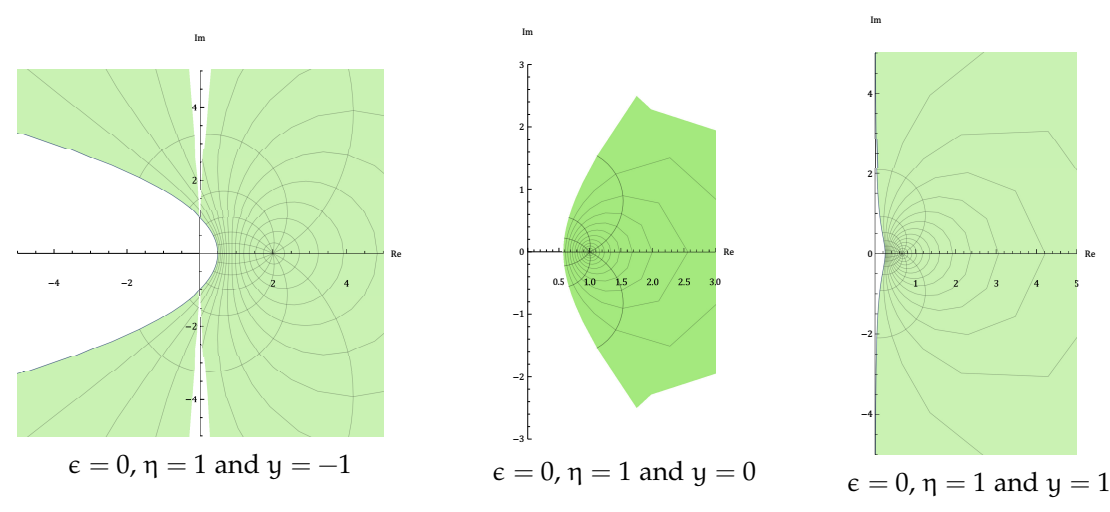


Figure 1: Image of  $\mathbb{D}$  under  $\mathfrak{J}_{i}(y, z)$ .

Throughout this paper, unless otherwise mentioned, we assume that

$$\kappa_{\mathbf{j}} := 1 + (\mathbf{j} - 1) (\mathbf{v} + \mathbf{t}) + (\mathbf{j}^2 + 1) \mathbf{v} \mathbf{t}, \quad \mathbf{j} \in \mathbb{N},$$

where  $v\geqslant 0$  and  $t\in [0,1].$  It is evident that  $\kappa_j$  is a real number such that  $\kappa_j\geqslant 1$ , and

$$\kappa_{j+1}-\kappa_j=\big(1+(2j+1)\,\mathtt{t}\big)\mathtt{v}+\mathtt{t}\geqslant 0.$$

For every  $h \in A$ , we define

$$\Lambda_{\mathtt{v},\mathtt{t}}\left(\mathtt{h}(z)\right) := (1-\mathtt{v})(1-\mathtt{t})\frac{\mathtt{h}(z)}{\mathtt{v}} + \left(\mathtt{t} + \mathtt{v}(1+\mathtt{t})\right)\mathtt{h}'(z) + \mathtt{v}\mathtt{t}(z\mathtt{h}''(z) - 2).$$

If  $h \in A$  is of the form  $h(z) = z + \sum_{j=2}^{\infty} u_j z^j$ , we have

$$\Lambda_{\text{v,t}}\left(\mathbf{h}(z)\right) = 1 + \sum_{j=2}^{\infty} \kappa_{j} u_{j} z^{j-1}.$$

With the aid of Jacobi polynomials, we define the subclasses of  $\sigma$  using the notion of subordination.

**Definition 1.1.** A function  $f \in \sigma$  is said to be in the class  $\mathcal{A}_{\sigma}^{(\varepsilon,\eta)}(v,t;y)$ , if

$$\Lambda_{\mathtt{v},\mathtt{t}}\left(\mathtt{f}(z)\right) \prec \mathfrak{J}_{\mathtt{j}}(\mathtt{y},z), \quad (z \in \mathbb{D}), \quad \text{and} \quad \Lambda_{\mathtt{v},\mathtt{t}}\left(\mathtt{f}^{-1}(w)\right) \prec \mathfrak{J}_{\mathtt{j}}(\mathtt{y},w), \quad (w \in \mathbb{D}),$$

where 
$$f^{-1}(w) = w + \sum_{j=2}^{\infty} v_j w^j$$
.

*Remark* 1.2. For t=0 and  $v\geqslant 1$ ,  $f\in \sigma$  is in the class  $\mathcal{A}_{\sigma}^{(\varepsilon,\eta)}(v,0;y)$ , if

$$\Lambda_{v,0}(f(z)) \prec \mathfrak{J}_{j}(y,z)$$
 and  $\Lambda_{v,0}(f^{-1}(w)) \prec \mathfrak{J}_{j}(y,z)$ .

Remark 1.3. For t=0 and v=1,  $f\in\sigma$  is in the class  $\mathcal{A}_{\sigma}^{(\varepsilon,\eta)}(1,0;y)$ , if

$$\Lambda_{1,0}(\mathbf{f}(z)) \prec \mathfrak{J}_{\mathbf{j}}(\mathbf{y},z)$$
 and  $\Lambda_{1,0}(\mathbf{f}^{-1}(w)) \prec \mathfrak{J}_{\mathbf{j}}(\mathbf{y},z)$ .

#### 2. The coefficient bounds

**Theorem 2.1.** If f(z), given by (1.1), is in  $\mathcal{A}_{\sigma}^{(\epsilon,\eta)}(v,t;y)$ , then

$$|\tau_2|\leqslant \frac{\left|\mathcal{N}_1^{(\varepsilon,\eta)}(y)\right|^{\frac{3}{2}}}{\sqrt{\left|\left(\mathcal{N}_1^{(\varepsilon,\eta)}(y)\right)^2\kappa_3-\mathcal{N}_2^{(\varepsilon,\eta)}(y)\kappa_2^2\right|}}\quad \text{and} \quad |\tau_3|\leqslant \frac{\left|\mathcal{N}_1^{(\varepsilon,\eta)}(y)\right|}{\kappa_3}+\frac{\left|\mathcal{N}_1^{(\varepsilon,\eta)}(y)\right|^2}{\kappa_2^2},$$

where  $\mathfrak{N}_{i}^{(\,\varepsilon,\eta\,)}(y),\;j=1,2$  are as in (1.2).

*Proof.* Since  $f \in \mathcal{A}_{\sigma}^{(\varepsilon,\eta)}(v,t;y)$ , there exist two analytic functions  $\gamma,\delta:\mathbb{D}\to\mathbb{D}$  given by

$$\gamma(z) = \sum_{j=1}^{\infty} \gamma_j z^j$$
 and  $\delta(w) = \sum_{j=1}^{\infty} \delta_j w^j$ 

with  $\gamma(0) = \delta(0) = 0$ ,  $|\gamma(z)| < 1$ ,  $|\delta(w)| < 1$  for all  $z, w \in \mathbb{D}$  such that

$$\Lambda_{v,t}(f(z)) = \mathfrak{J}_{j}(y,\gamma(z)) \quad \text{and} \quad \Lambda_{v,t}(f^{-1}(w)) = \mathfrak{J}_{j}(y,\delta(w)).$$

Or equivalently

$$1 + \sum_{j=2}^{\infty} \kappa_{j} \tau_{j} z^{j-1} = 1 + \mathcal{N}_{1}^{(\epsilon,\eta)}(y) \gamma_{1} z_{1} + \left[\mathcal{N}_{1}^{(\epsilon,\eta)}(y) \gamma_{2} + \mathcal{N}_{2}^{(\epsilon,\eta)}(y) \gamma_{1}^{2}\right] z^{2}$$

$$\times \left[\mathcal{N}_{2}^{(\epsilon,\eta)}(y) \gamma_{1} \gamma_{2} + \mathcal{N}_{1}^{(\epsilon,\eta)}(y) \gamma_{3} + \mathcal{N}_{3}^{(\epsilon,\eta)} \gamma_{1}^{3}\right] z^{3} + \cdots$$

$$(2.1)$$

and

$$1 + \sum_{j=2}^{\infty} \kappa_{j} \tau_{j} w^{j-1} = 1 + \mathcal{N}_{1}^{(\epsilon,\eta)}(y) \delta_{1} w_{1} + \left[ \mathcal{N}_{1}^{(\epsilon,\eta)}(y) \delta_{2} + \mathcal{N}_{2}^{(\epsilon,\eta)}(y) \delta_{1}^{2} \right] w^{2}$$

$$\times \left[ \mathcal{N}_{2}^{(\epsilon,\eta)}(y) \delta_{1} \delta_{2} + \mathcal{N}_{1}^{(\epsilon,\eta)}(y) \delta_{3} + \mathcal{N}_{3}^{(\epsilon,\eta)} \delta_{1}^{3} \right] w^{3} + \cdots$$

$$(2.2)$$

Since  $|\gamma(z)| < 1$  and  $|\delta(w)| < 1$ , it is clear that  $|\gamma_j| \le 1$ ,  $|\delta_j| \le 1$ , for  $j = 1, 2, \ldots$  From (2.1) and (2.2), we have

$$\kappa_2 \tau_2 = \mathcal{N}_1^{(\varepsilon, \eta)}(y) \gamma_1, \tag{2.3}$$

$$\kappa_3\tau_3 = \mathcal{N}_1^{(\varepsilon,\eta)}(y)\gamma_2 + \mathcal{N}_2^{(\varepsilon,\eta)}(y)\gamma_1^2, \tag{2.4}$$

$$-\kappa_2 \tau_2 = \mathcal{N}_1^{(\epsilon, \eta)}(y) \delta_1, \tag{2.5}$$

and

$$\kappa_3(2\tau_2^2 - \tau_3) = \mathcal{N}_1^{(\varepsilon,\eta)}(y)\delta_2 + \mathcal{N}_2^{(\varepsilon,\eta)}(y)\delta_1^2. \tag{2.6}$$

From (2.3) and (2.5), we can easily see that

$$\gamma_1 = -\delta_1,\tag{2.7}$$

$$2\kappa_2^2 \tau_2^2 = [\mathcal{N}_1^{(\epsilon, \eta)}(y)]^2 [\gamma_1^2 + \delta_1^2]. \tag{2.8}$$

Upon adding (2.4) and (2.6), we get

$$2\kappa_3\tau_2^2 = \mathcal{N}_1^{(\varepsilon,\eta)}(y)(\gamma_2 + \delta_2) + \mathcal{N}_2^{(\varepsilon,\eta)}(y)(\gamma_1^2 + \delta_1^2). \tag{2.9}$$

By using (2.8) in (2.9), we have

$$2\left[\kappa_3\left(\mathcal{N}_1^{(\varepsilon,\eta)}(y)\right)^2 - \kappa_2^2\mathcal{N}_2^{(\varepsilon,\eta)}(y)\right]\tau_2^2 = \left(\mathcal{N}_1^{(\varepsilon,\eta)}(y)\right)^3(\gamma_2 + \delta_2), \tag{2.10}$$

which implies

$$|\tau_2|\leqslant \frac{\left|\mathcal{N}_1^{(\varepsilon,\eta)}(y)\right|^{\frac{3}{2}}}{\sqrt{\left|\left(\mathcal{N}_1^{(\varepsilon,\eta)}(y)\right)^2\kappa_3-\mathcal{N}_2^{(\varepsilon,\eta)}(y)\kappa_2^2\right|}}.$$

Upon subtracting (2.6) from (2.4) and using (2.7), we get

$$\tau_3 - \tau_2^2 = \frac{\mathcal{N}_1^{(\epsilon, \eta)}(y)(\gamma_2 - \delta_2)}{2\kappa_3}.$$
 (2.11)

Then, in aid of (2.8), we get

$$\tau_3 = \frac{\mathcal{N}_1^{(\varepsilon,\eta)}(y)(\gamma_2 - \delta_2)}{2\kappa_3} + \frac{[\mathcal{N}_1^{(\varepsilon,\eta)}(y)]^2(\gamma_1^2 + \delta_1^2)}{2\kappa_2^2}.$$

Thus

$$|\tau_3| \leqslant \frac{\left|\mathcal{N}_1^{(\varepsilon,\eta)}(y)\right|}{\kappa_3} + \frac{\left|\mathcal{N}_1^{(\varepsilon,\eta)}(y)\right|^2}{\kappa_2^2}.$$

**Corollary 2.2.** If f(z), given by (1.1), is in  $\mathcal{A}_{\sigma}^{(\epsilon,\eta)}(v,0;y)$ , then

$$|\tau_2|\leqslant \frac{\left|\mathcal{N}_1^{(\varepsilon,\eta)}(y)\right|^{\frac{3}{2}}}{\sqrt{\left|\left(\mathcal{N}_1^{(\varepsilon,\eta)}(y)\right)^2\left(1+2v\right)-\mathcal{N}_2^{(\varepsilon,\eta)}(y)\left(1+v\right)^2\right|}}\quad \text{and} \quad |\tau_3|\leqslant \frac{\left|\mathcal{N}_1^{(\varepsilon,\eta)}(y)\right|}{1+2v}+\frac{\left|\mathcal{N}_1^{(\varepsilon,\eta)}(y)\right|^2}{(1+v)^2},$$

where  $\mathcal{N}_{j}^{(\varepsilon,\eta)}(y)$ , j=1,2 are as in (1.2).

**Corollary 2.3.** If f(z), given by (1.1), is in  $\mathcal{A}_{\sigma}^{(\epsilon,\eta)}(1,0;y)$ , then

$$|\tau_2|\leqslant \frac{\left|\mathcal{N}_1^{(\varepsilon,\eta)}(y)\right|^{\frac{3}{2}}}{\sqrt{\left|3\left(\mathcal{N}_1^{(\varepsilon,\eta)}(y)\right)^2-4\mathcal{N}_2^{(\varepsilon,\eta)}(y)\right|}}\quad \textit{and} \quad |\tau_3|\leqslant \frac{\left|\mathcal{N}_1^{(\varepsilon,\eta)}(y)\right|}{3}+\frac{\left|\mathcal{N}_1^{(\varepsilon,\eta)}(y)\right|^2}{4},$$

where  $\mathfrak{N}_{j}^{(\varepsilon,\eta)}(y)$ , j=1,2 are as in (1.2).

#### 3. Fekete-Szegö inequalities

**Theorem 3.1.** If f(z), given by (1.1), is in  $\mathcal{A}_{\sigma}^{(\varepsilon,\eta)}(v,t;y)$  and  $\rho \in \mathbb{R}$ , then

$$|\tau_3-\rho\tau_2^2|\leqslant\begin{cases}\frac{|\mathcal{N}_1^{(\varepsilon,\eta)}(y)|}{\kappa_3}, & 0\leqslant|\Xi(\mathtt{v},\mathtt{t})|\leqslant\frac{1}{2\kappa_3},\\2|\mathcal{N}_1^{(\varepsilon,\eta)}(y)\Xi(\mathtt{v},\mathtt{t})|, & |\Xi(\mathtt{v},\mathtt{t})|\geqslant\frac{1}{2\kappa_3}.\end{cases}$$

*Proof.* For  $\rho \in \mathbb{R}$  and from (2.11), we have

$$\tau_{3} - \rho \tau_{2}^{2} = \frac{\mathcal{N}_{1}^{(\epsilon, \eta)}(y)(\gamma_{2} - \delta_{2})}{2\kappa_{3}} + (1 - \rho)\tau_{2}^{2}.$$

By using (2.10), we get

$$\begin{split} \tau_3 - \rho \tau_2^2 &= \frac{\mathcal{N}_1^{(\varepsilon,\eta)}(y)(\gamma_2 - \delta_2)}{2\kappa_3} + (1 - \rho) \left( \frac{\left(\mathcal{N}_1^{(\varepsilon,\eta)}(y)\right)^3 (\gamma_2 + \delta_2)}{2[\kappa_3 \left(\mathcal{N}_1^{(\varepsilon,\eta)}(y)\right)^2 - \kappa_2^2 \mathcal{N}_2^{(\varepsilon,\eta)}(y)]} \right) \\ &= \mathcal{N}_1^{(\varepsilon,\eta)}(y) \left[ \left( \frac{1}{2\kappa_3} + \Xi(v,t) \right) \gamma_2 + \left( \frac{-1}{2\kappa_3} + \Xi(v,t) \right) \delta_2 \right], \end{split}$$

$$\text{where }\Xi(\mathtt{v},\mathtt{t}) = \frac{(1-\rho)[\mathcal{N}_1^{(\varepsilon,\eta)}(\mathtt{y})]^2}{2[\kappa_3\left(\mathcal{N}_1^{(\varepsilon,\eta)}(\mathtt{y})\right)^2 - \kappa_2^2\mathcal{N}_2^{(\varepsilon,\eta)}(\mathtt{y})]}. \text{ Thus}$$

$$|\tau_3 - \rho \tau_2^2| \leqslant \begin{cases} \frac{|\mathcal{N}_1^{(\varepsilon,\eta)}(y)|}{\kappa_3}, & 0 \leqslant |\Xi(v,t)| \leqslant \frac{1}{2\kappa_3}, \\ 2|\mathcal{N}_1^{(\varepsilon,\eta)}(y)\Xi(v,t)|, & |\Xi(v,t)| \geqslant \frac{1}{2\kappa_3}. \end{cases}$$

**Corollary 3.2.** *If* f(z), given by (1.1), is in  $\mathcal{A}_{\sigma}^{(\varepsilon,\eta)}(v,0;y)$  and  $\rho \in \mathbb{R}$ , then

$$\begin{split} |\tau_3 - \rho \tau_2^2| \leqslant \begin{cases} \frac{|\mathcal{N}_1^{(\varepsilon, \eta)}(y)|}{1 + 2v}, & 0 \leqslant |\Xi(v, 0)| \leqslant \frac{1}{2(1 + 2v)}, \\ 2|\mathcal{N}_1^{(\varepsilon, \eta)}(y)\Xi(v, 0)|, & |\Xi(v, 0)| \geqslant \frac{1}{2(1 + 2v)}. \end{cases} \end{split}$$

$$\textit{where}\ \Xi(v,0) = \frac{(1-\rho)[\mathcal{N}_1^{(\varepsilon,\eta)}(y)]^2}{2[(1+2v)\left(\mathcal{N}_1^{(\varepsilon,\eta)}(y)\right)^2 - (1+v)^2\,\mathcal{N}_2^{(\varepsilon,\eta)}(y)]}.$$

**Corollary 3.3.** *If* f(z), given by (1.1), is in  $\mathcal{A}_{\sigma}^{(\varepsilon,\eta)}(1,0;y)$  and  $\rho \in \mathbb{R}$ , then

$$|\tau_3-\rho\tau_2^2|\leqslant\begin{cases}\frac{|\mathcal{N}_1^{(\varepsilon,\eta)}(y)|}{3}, & 0\leqslant|\Xi(\textbf{1},\textbf{0})|\leqslant\frac{1}{6},\\2|\mathcal{N}_1^{(\varepsilon,\eta)}(y)\Xi(\textbf{1},\textbf{0})|, & |\Xi(\textbf{1},\textbf{0})|\geqslant\frac{1}{6}.\end{cases}$$

where 
$$\Xi(1,0) = \frac{(1-\rho)[\mathcal{N}_1^{(\epsilon,\eta)}(y)]^2}{2[3\left(\mathcal{N}_1^{(\epsilon,\eta)}(y)\right)^2 - 4\mathcal{N}_2^{(\epsilon,\eta)}(y)]}.$$

#### 4. Applications

Image enhancement is a systematic process aimed at improving the visual quality and interpretability of digital images. The procedure typically begins with image acquisition, followed by preprocessing steps designed to prepare the image for enhancement. Based on the image's characteristics and the desired outcome, an appropriate enhancement technique is selected. These methods can operate in the spatial domain, frequency domain, or leverage a hybrid approach that combines elements of both.

In this study, the primary focus is on Spatial Domain Techniques, where an image is often modeled as a  $2 \times 2$  matrix, with each element representing the intensity of an individual pixel. These techniques are mathematically formulated as: v(x,y) = T[u(x,y)], where u(x,y) denotes the original input image, v(x,y) represents the enhanced image, and T is an operator applied to the neighborhood of pixel (x,y). This operator may act on a single image or multiple images depending on the specific enhancement task.

A fundamental operation in spatial domain enhancement is convolution, a core mathematical process widely used in image processing. Convolution integrates a small filter (or kernel) with the image to produce a transformed output, where each pixel in the resulting image is a linear combination of neighboring pixel values from the input, weighted by the kernel. This mechanism forms the basis for various enhancement tasks, such as blurring, sharpening, and edge detection.

In critical domains such as medical imaging and computer vision, particularly in applications like retinal image analysis or edge detection, image enhancement plays a pivotal role in improving diagnostic accuracy and visual clarity. This work proposes a novel enhancement technique grounded in a mathematical framework inspired by Geometric Function Theory (GFT). Specifically, it utilizes coefficient bounds derived from GFT and applies them through convolution to the input image. This method aims to achieve significant improvements in contrast, brightness, and structural fidelity.

To rigorously evaluate the performance of the proposed enhancement method, several established image quality metrics are employed. These include following.

- Peak Signal-to-Noise Ratio (PSNR): Quantifies the fidelity of the enhanced image relative to the original, with higher values indicating better quality.
- Structural Similarity Index Measure (SSIM): Assesses the perceptual similarity between the original and enhanced images by evaluating luminance, contrast, and structural information.
- Pearson Correlation Coefficient (PCC): Measures the linear correlation between pixel intensities of the original and enhanced images, indicating the strength and direction of association.

The integration of GFT-based convolution with these performance metrics ensures that the proposed method not only improves visual aesthetics but also maintains essential structural and diagnostic information, making it highly suitable for analytical and interpretive tasks in both research and clinical contexts.

Recent research in geometric function theory (GFT) highlights its growing significance in advancing image enhancement techniques, complementing established approaches like deep learning, fractional methods, and fuzzy logic (see [1, 11]. Notable studies demonstrate GFT's potential in this domain. Nithiyanandham et al. [10] introduced the class  $p - \xi S^*(t, \mu, \nu, J, K)$ , derived from a Mittag-Leffler-type Poisson distribution, to analyze coefficient bounds, achieving significant improvements in retinal image enhancement. Nandhini et al. [9] enhanced image quality using a subclass of analytic functions integrating the Mittag-Leffler-type Poisson distribution with starlike functions. Their approach was validated on the Flower Image Dataset and the Brain-Stroke-Prediction CT Scan Image Dataset, demonstrating robust performance. Sivagami Sundari et al. [18] utilized a Sakaguchi-type function subordinated with Gegenbauer polynomials for low-light image enhancement. However, this method faces challenges with unevenly illuminated images, often resulting in over-enhancement in brighter regions.

These studies emphasize the critical role of coefficient bounds in optimizing image enhancement outcomes. Despite these advancements, the application of Jacobi polynomials within GFT for image enhancement remains underexplored. Only a few researchers [2, 3] have combined bi-univalent functions

with Jacobi polynomials to explore their theoretical aspects. In this work, we introduce a novel subclass of bi-univalent functions associated with Jacobi polynomials, marking a pioneering contribution to the literature. Our proposed subclass exhibits superior properties compared to existing methods, enhancing the efficacy of image processing techniques.

Our research focuses on developing image enhancement algorithms based on the convolution of coefficient bounds derived from this novel subclass of bi-univalent functions. These algorithms demonstrate significant potential in digital image processing applications, achieving optimal results as detailed in our findings.

#### 4.1. Jacobi polynomial convolution enhancement algorithm (JPCEA)

In this section, we present a rigorous mathematical formulation based on the coefficients derived for the function class defined as  $\mathcal{A}_{\sigma}^{(\varepsilon,\eta)}(v,t;y)$ . As we proved in Section 2, these coefficients, denoted by  $\tau_n$ , were calculated using the Jacobi polynomials and serve as the foundation for the image enhancement process.

The image enhancement is performed through a convolutional operation in which the original image is processed using the set of derived coefficients. Let the enhanced image be represented as  $\mathfrak{I}_{\mathfrak{E}}(\mathfrak{m},\mathfrak{n})$ . It is obtained via the following convolution formula:  $\mathfrak{I}_{\mathfrak{E}}(\mathfrak{m},\mathfrak{n})=\mathfrak{M}*\mathfrak{I}(\mathfrak{m},\mathfrak{n})$ , where  $\mathfrak{M}$  is the mask window in  $3\times 3$  matrix,  $\mathfrak{I}(\mathfrak{m},\mathfrak{n})$  represents the coefficients of the original image, and  $\mathfrak{I}_{\mathfrak{E}}(\mathfrak{m},\mathfrak{n})$  represents the coefficients of the enhanced image. The mask window coefficients  $\tau_1,\tau_2,\tau_3$  are represented in the  $3\times 3$  matrices as follows:

$$0^{\circ} = \begin{bmatrix} 0 & 0 & 0 \\ \tau_{1} & \tau_{2} & \tau_{3} \\ 0 & 0 & 0 \end{bmatrix} \qquad 90^{\circ} = \begin{bmatrix} \tau_{3} & 0 & 0 \\ 0 & \tau_{2} & 0 \\ 0 & 0 & \tau_{1} \end{bmatrix} \qquad 45^{\circ} = \begin{bmatrix} \tau_{3} & 0 & 0 \\ \tau_{2} & 0 & 0 \\ \tau_{1} & 0 & 0 \end{bmatrix} \qquad 135^{\circ} = \begin{bmatrix} \tau_{3} & 0 & 0 \\ 0 & \tau_{2} & 0 \\ 0 & 0 & \tau_{1} \end{bmatrix}$$

For v = 0, t = 1, the coefficients are defined as:

$$\tau_1=1,\quad \tau_2=\frac{\left|\mathcal{N}_1^{(\varepsilon,\eta)}(y)\right|^{\frac{3}{2}}}{\sqrt{\left|3\left(\mathcal{N}_1^{(\varepsilon,\eta)}(y)\right)^2-4\mathcal{N}_2^{(\varepsilon,\eta)}(y)\right|}},\quad \tau_3=\frac{\left|\mathcal{N}_1^{(\varepsilon,\eta)}(y)\right|}{3}+\frac{\left|\mathcal{N}_1^{(\varepsilon,\eta)}(y)\right|^2}{4}.$$

We will enhance the images for the above values of the coefficients with suitable parameters (y = 1,  $\varepsilon = -0.7$ , and  $\eta = -0.51$ ). The outputs for image enhancement using the bi-univalent function are obtained from the following algorithm.

- 1. Read an image from the specified file path.
- 2. Convert the image to grayscale.
- 3. Define functions to create convolution masks for different angles  $0^{\circ}$ ,  $45^{\circ}$ ,  $90^{\circ}$ , and  $135^{\circ}$ .
- 4. Define the coefficients for the masks  $(\tau_1, \tau_2, \tau_3)$ .
- 5. Apply each mask to the grayscale image using the convolution operation.
- 6. Calculate the average of the resulting images obtained from different angles.
- 7. Visualize the original grayscale image, the edge-detected images at different angles, and the average of the edge-detected images.

#### 5. Experimental findings and analysis

The effectiveness of image enhancement is shown below for various images. For this purpose, we used RGB images "Albert" of size  $500 \times 460$ , "Foot X-ray" of dimensions  $1077 \times 2029$ , "Covid19" of pixel size  $649 \times 520$ , and "Bee Hummingbird" of dimension  $1024 \times 576$ , respectively. The following RGB images are converted to grayscale. Subsequently, these images were further enhanced using a subclass of analytic functions.

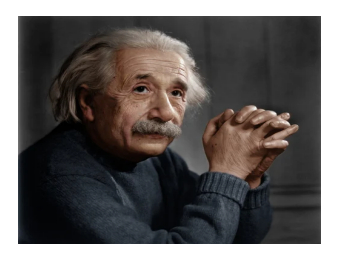


Figure 2: RGB image of "Albert Einstein".



Figure 3: RGB image of "Foot X-ray".

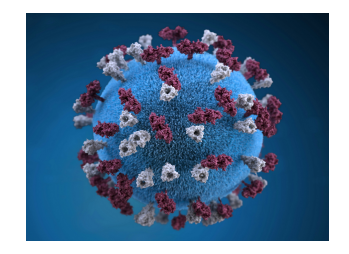


Figure 4: RGB image of "Covid19"



Figure 5: RGB image of "Bee Hummingbird"



Mask at 90 deg









Figure 6: Enhanced image of Albert Einstein at different mask angles.

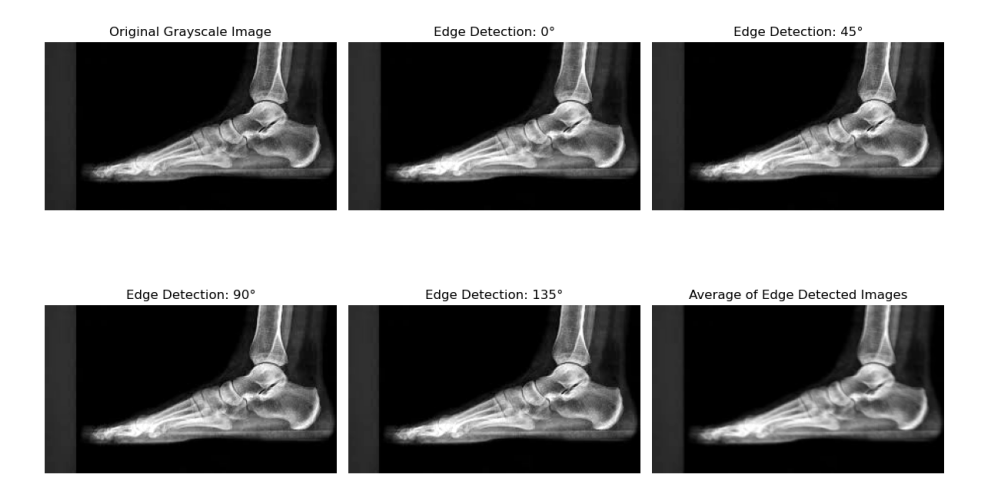


Figure 7: Enhanced image of Foot at different mask angles.

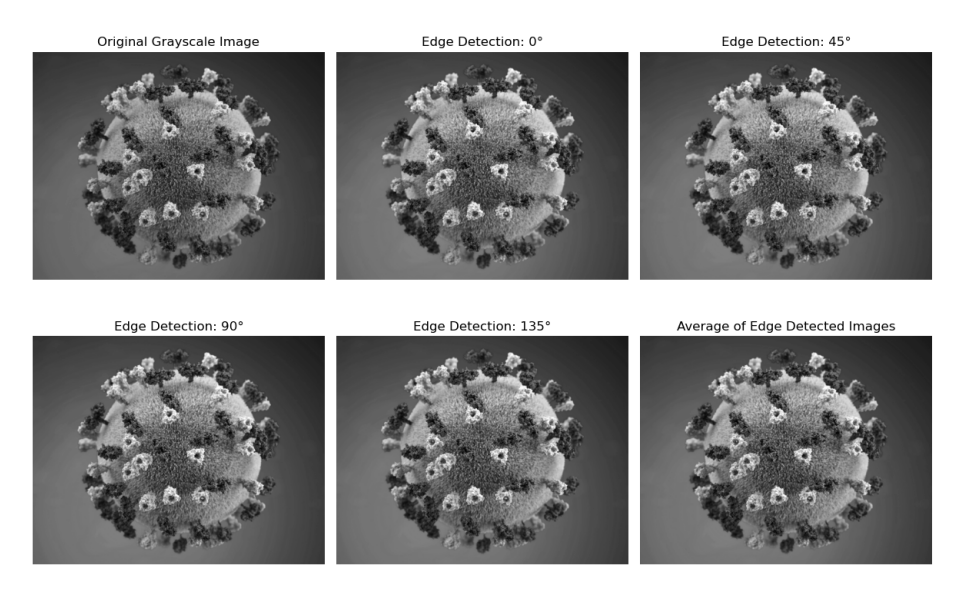


Figure 8: Enhanced image of Covid19 at different mask angles.

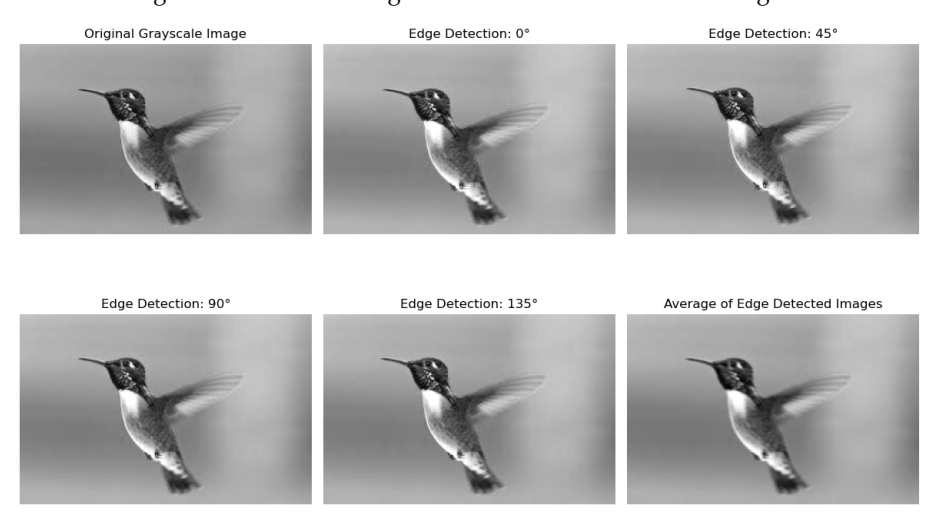


Figure 9: Enhanced image of Bee Hummingbird at different mask angles.

Table 2: The quality metric values (PSNR, SSIM, PCC) of the test images (Albert Einstein, Foot X-ray, Covid19, and Bee Hummingbird).

Image name	PSNR	SSIM	PCC
Albert Einstein (2)	24.91017212	0.92853638	0.99311384
Foot X-ray (3)	23.77993325	0.92661368	0.98775379
Covid19 (4)	23.68038280	0.97003575	0.99784904
Bee Hummingbird (5)	18.24548058	0.94618020	0.97281660

Table 3: Comparison of obtained PCC values and histogram equalization PCC values of the test images (Albert Einstein, Foot X-ray, Covid19, and Bee Hummingbird).

Image Name	PCC (JPCEA)	PCC (HISTOGRAM)	
Albert Einstein (2)	0.99311384	0.90013822	
Foot X-ray (3)	0.98775379	0.96064637	
Covid19 (4)	0.99784904	0.91977654	
Bee Hummingbird (5)	0.97281660	0.91041941	

### 6. Data availability

The following sources were used for the data in this research work: the source image of Albert Einstein, the source image of COVID-19, the source image of Foot X-ray, and the source image of Bee Hummingbird.

#### 7. Conclusion

We have estimated the bounds for  $|\tau_2|$  and  $|\tau_3|$ , and the Fekete-Szegö inequality for subclasses of bi-univalent functions subordinated to Jacobi polynomials. In this research work, our objective was to improve image quality through specific enhancements such as increasing brightness, contrast, and sharpness. We utilized Python OpenCV, an open-source library for performing various image enhancement techniques. The outcomes highlight the efficiency of this method in enhancing diverse images, proving its stability and flexibility. Through modifications of the parameters  $\varepsilon$ ,  $\eta$ , and y within the analytical framework, we expect our findings to have practical utility in areas such as image sharpening, edge detection, and advancing image resolution.

#### Acknowledgment

If you would like to thank anyone, place your comments here. Acknowledge any funding, assistance, or contributions that were instrumental to the completion of your research.

#### References

- [1] B. Aarthy, B. S. Keerthi, Enhancement of various images using coefficients obtained from a class of Sakaguchi type functions, Sci. Rep., 13 (2023), 14 pages. 4
- [2] A. Amourah, T. Al-Hawary, F. Yousef, J. Salah, Collection of bi-univalent functions using bell distribution associated with Jacobi polynomials, Int. J. Neutrosophic Sci., 25 (2025), 228–238. 4
- [3] A. Amourah, B. Frasin, J. Salah, F. Yousef, Subfamilies of Bi-Univalent Functions Associated with the Imaginary Error Function and Subordinate to Jacobi Polynomials, Symmetry, 17 (2025), 12 pages. 4
- [4] V. Balasubramaniam, S. Gunasekar, B. Sudharsanan, S. Yalçın, *Horadam polynomials for a new subclass of Sakaguchi-type bi-univalent functions defined by* (p, q)-*derivative operator*, Commun. Korean Math. Soc., **39** (2024), 461–470.
- [5] D. A. Brannan, J. Clunie, Aspects of contemporary complex analysis, Academic Press, (1980). 1
- [6] B. G. S. Doman, The classical orthogonal polynomials, World Scientific Publishing Co. Pte. Ltd., Hackensack, NJ, (2016). 1
- [7] N. N. Lebedev, Special functions and their applications, Prentice-Hall, Inc., Englewood Cliffs, NJ, (1965). 1
- [8] M. Lewin, On a coefficient problem for bi-univalent functions, Proc. Amer. Math. Soc., 18 (1967), 63-68. 1
- [9] B. Nandhini, B. Sruthakeerthi, *Investigating the quality measures of image enhancement by convoluting the coefficients of analytic functions*, Eur. Phys. J. Spec. Top., **234** (2025), 2647–2657. 4
- [10] E. K. Nithiyanandham, B. Srutha Keerthi, *A new proposed model for image enhancement using the coefficients obtained by a subclass of the Sakaguchi-type function*, Signal Image Video Process., **18** (2024), 1455–1462. 4
- [11] E. K. Nithiyanandham, B. Srutha Keerthi, *Image edge detection enhancement using coefficients of Sakaguchi type functions mapped onto petal shaped domain*, Heliyon, **10** (2024), 6 pages. 4
- [12] G. Saravanan, S. Baskaran, B. Vanithakumari, L. Alnaji, T. G. Shaba., I. Al-Shbeil, A. A. Lupas, *Bernoulli polynomials For a New subclass of Te-univalent functions*, Heliyon, **10** (2024), 11 pages 1
- [13] G. Saravanan, S. Baskaran, B. Vanithakumari, A. K. Wanas, *Gegenbauer polynomials for a new subclass of bi-univalent functions*, Kyungpook Math. J., **64** (2024), 487–497.
- [14] T. G. Shaba, S. Araci, B. O. Adebesin, *Application of Three Leaf Domain on a Subclass of Bi-univalent Functions*, In: 2024 International Conference on Science, Engineering and Business for Driving Sustainable Development Goals (SEB4SDG), IEEE, 2024, 1–7.
- [15] T. G. Shaba, S. Araci, B. O. Adebesin, F. Usta, B. Khan, *Characterization of Bi-Starlike Functions: A Daehee Polynomial Approach*, Symmetry, **16** (2024), 16 pages.
- [16] T. G. Shaba, F. M. O. Tawfiq, D. Breaz, L.-I. Cotîrl a, New Uses of q-Generalized Janowski Function in q-Bounded Turning Functions, Mathematics, 12 (2024), 19 pages.
- [17] T. G. Shaba, S. Yalçin, G. Murugusundaramoorthy, M. Darus, *Certain Subclasses of Bi-univalent Functions Associated with (u, v)-Chebyshev Polynomials.*, Appl. Math. J. Chinese Univ. Ser. B, **40** (2025), 429–442. 1

- [18] K. S. Sundari, B. S. Keerthi, Enhancing low-light images using Sakaguchi type function and Gegenbauer polynomial, Sci. Rep., 14 (2024), 1–14. 4
- [19] Q.-H. Xu, Y.-C. Gui, H. M. Srivastava, Coefficient estimates for a certain subclass of analytic and bi-univalent functions, Appl. Math. Lett., 25 (2012), 990–994. 1